International Journal of Innovative
Computing, Information and Control
Volume **17**, Number **5**, October **2021**

 ISSN 1349-4198
pp. 1745–1762

CALCULATION METHOD FOR THE RESPONSE PATTERNS OF A CASCADE MODEL USING ITS RECURSIVE PROPERTY

Kohichi Ogata

Faculty of Advanced Science and Technology
Kumamoto University
2-39-1 Kurokami, Chuo-ku, Kumamoto 860-8555, Japan
ogata@cs.kumamoto-u.ac.jp

Received April 2021; revised July 2021

Abstract. *This paper describes a useful calculation method for the response patterns of a model comprising a cascaded first-order system. In the modeling, the impulse response of the model was used to describe the velocity pattern of the movement. The differentiation and integration of the impulse response were analyzed by focusing on the recursive structure involving impulse responses with different orders. Response patterns, such as displacement, velocity, and acceleration, can be calculated based on the properties of the model and its recursive property, and these patterns can be described as a combination of the impulse response patterns. The effectiveness of the calculation method was also validated for the calculation of a gamma function. Moreover, to verify the flexibility of the modeling method, the visualization of the patterns based on the calculation method was demonstrated for an intuitive understanding of waveform modeling for displacement, velocity, and acceleration. The method provides a new perspective on the modeling and analysis of response patterns in the approximation of the transfer functions for high-order systems using a cascade model.*

Keywords: Cascaded first-order system, Approximation model, Recursive calculation, Gamma function, Impulse response, Trajectory pattern

1. **Introduction.** Simple models for high-order systems provide useful approximations for complex transfer functions. As an example of one of these approximation models, a model comprising a cascaded first-order system was introduced, and the properties of the n-th cascade of equal-time-constant systems were established in [1]. Based on this idea, a model consisting of a cascaded first-order system was applied to the representation of articulatory behavior [2, 3, 4, 5]. In this approach, the impulse response of the 10-th order cascaded first-order system was used to represent the velocity profile of articulatory behavior, such as tongue, lip, and jaw movement patterns. Given that the impulse response patterns provide an optimal approximation for the velocity profile, the displacement, velocity, and acceleration of the movement patterns were accurately represented using the response of the model. The effectiveness of the model for articulatory trajectories was also reported in [6] based on [3, 5].

To determine the basic components from the measured waveforms, other methods such as the principal component analysis (PCA) [7, 8] and independent component analysis (ICA) [9, 10] can be considered. In PCA, the observed data are decomposed into orthogonal components corresponding to mutually orthogonal principal axes. PCA is useful for the dimension reduction and can efficiently control the behavior of data using a linear combination of principal components. In ICA, the observed data are decomposed into statistically independent non-Gaussian source signals. This method provides a source-signal

DOI: 10.24507/ijicic.17.05.1745

separation without information about transfer functions. Although ICA is a powerful decomposition method, problems regarding the indeterminacy of permutation and scaling should be considered. A relatively recent study [11] also proposed a method to overcome the permutation problem, that is, the channel selection problem, in the development of a real-time blind source separation for human speech signals. Although these methods have the potential to determine the basic components, they require calculation costs and special attention to the data processing such as permutation.

In contrast, if we can determine a simple explicit function model that can effectively represent the response patterns of systems, the response patterns of the model can be used as the basic components of waveforms. Furthermore, if the model can produce smooth and continuous waveform patterns, the flexibility of the model for representing complex response patterns by combining several response patterns is also expected. The simplicity and flexibility of the model contribute to simple and effective waveform modeling and control with a low calculation cost.

This study aimed to demonstrate the properties of a model consisting of a cascaded first-order system, and to propose a method for calculating the response patterns based on the model's recursive property. Interestingly, these properties allow us to calculate the integration and differentiation of the impulse response pattern by combining the impulse response patterns of the models with different orders. The practicality of the calculation method based on its recursive property is also validated for the calculation of a gamma function.

In this paper, Section 2 describes a cascade model consisting of n units of a first-order component, and its transfer function and impulse response. In Section 3, a model based on a cascade model for articulatory movements is introduced. Section 4 focuses on the recursive property of the cascade model. The integration and differentiation of the impulse response pattern can be obtained by combining the impulse response patterns with different orders. Section 5 demonstrates an application of the calculation method to the gamma function. As a demonstration, Section 6 provides waveform modeling for displacement, velocity, and acceleration to visualize the generated patterns and demonstrate the flexibility of the modeling method. Section 7 discusses the outcomes of this study and its expected benefits. Finally, the conclusions of this study are presented in Section 8.

2. **Cascaded First-Order System [1].** Equation (1) expresses the transfer function of a model consisting of n units of a first-order component with an equal time constant, T:

$$H(s) = \frac{1}{(1+sT)^n} \tag{1}$$

Its impulse response is given as follows:

$$h(t) = \frac{1}{(n-1)!T}\left(\frac{t}{T}\right)^{n-1} e^{-\frac{t}{T}}, \quad t \geq 0 \tag{2}$$

Figure 1 presents the impulse response patterns for the variation of the order n ranging from 1 to 6 as examples. The configuration of the cascade model is presented in the upper part of the figure. The patterns have an interesting feature in which the n-th order impulse response pattern has its maximum value at $(n-1)T$ and simultaneously, the $(n-1)$-th order impulse response pattern crosses the maximum value point for the n-th order pattern.

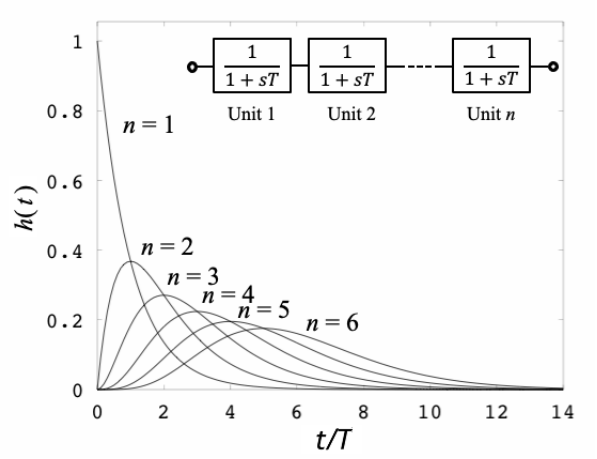

FIGURE 1. Impulse responses of the cascade model

3. **Modeling Based on a Cascaded First-Order System.** This section briefly describes the basic idea of articulatory modeling based on a cascaded first-order system [2, 4]. In the modeling process, the following impulse response was used to represent the time pattern of articulatory behavior:

$$h_n(t) = \frac{A}{(n-1)!T}\left(\frac{t}{T}\right)^{n-1} e^{-\frac{t}{T}}, \quad t \geq 0 \tag{3}$$

where A is the amplitude of the displacement.

Figure 2 schematically represents articulatory movement patterns based on a step response of the cascade. The patterns are presented in terms of displacement, velocity, and acceleration. In this example, a step input as a hypothetical motor command to the cascade model produces ascending movement, as shown in the top of the figure. Equivalently, the impulse response defined by Equation (3) corresponds to the velocity pattern. The displacement time pattern was calculated by integrating the velocity patterns. Moreover, the acceleration time pattern was calculated by differentiating the velocity patterns. As illustrated in Figure 2, the amplitude A corresponds to the displacement of the movement. Articulatory behavior consisting of successive movements is represented by combining the step-response patterns produced by sequential hypothetical motor commands [2].

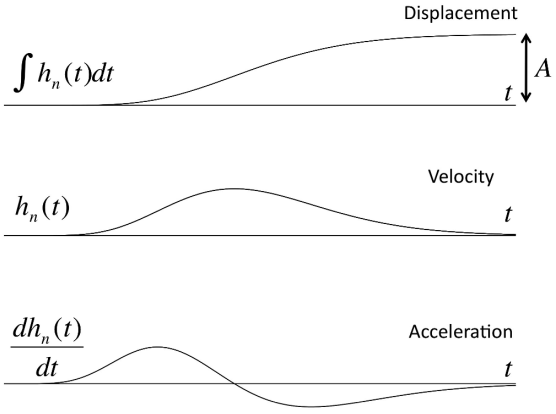

FIGURE 2. Modeling of articulatory movements based on a cascade model

4. **Properties of the Model Consisting of a First-Order System.** The time patterns, i.e., waveforms for the displacement and acceleration for articulatory modeling in the previous section, are obtained via numerical integration and the differentiation of Equation (3), respectively. However, these patterns can be calculated by focusing on the recursive properties of the cascade model, as described below.

4.1. Calculation based on recursive property.

4.1.1. *Differentiation.* By differentiating Equation (3) relative to t, the following equation can be obtained:

$$\begin{aligned}\frac{dh_n(t)}{dt} &= \frac{A}{(n-1)!T}\left\{(n-1)\left(\frac{t}{T}\right)^{n-2}\frac{1}{T}e^{-\frac{t}{T}} - \left(\frac{t}{T}\right)^{n-1}\frac{1}{T}e^{-\frac{t}{T}}\right\} \\ &= \frac{1}{T}\left\{\frac{A}{(n-2)!T}\left(\frac{t}{T}\right)^{n-2}e^{-\frac{t}{T}} - \frac{A}{(n-1)!T}\left(\frac{t}{T}\right)^{n-1}e^{-\frac{t}{T}}\right\} \\ &= \frac{1}{T}\left\{h_{n-1}(t) - h_n(t)\right\} \end{aligned} \tag{4}$$

This result suggests that the derivative of Equation (3), relative to t, consists of a combination of the n-th and $(n-1)$-th impulse response patterns based on Equation (3). High-order derivatives can also be obtained in the same manner. Therefore, the impulse response pattern given by Equation (3) can be considered a fundamental component of the derivatives.

Figure 3 presents a visual description of the derivative of Equation (3). As illustrated in the figure, the waveform of the derivative is formed by combining two impulse response patterns based on Equation (3). Regarding the second-order derivative, the following equation can be obtained:

$$\frac{d}{dt}\left(\frac{dh_n(t)}{dt}\right) = \frac{d}{dt}\left\{\frac{1}{T}\left\{h_{n-1}(t) - h_n(t)\right\}\right\} = \frac{1}{T}\left\{\frac{dh_{n-1}(t)}{dt} - \frac{dh_n(t)}{dt}\right\} \tag{5}$$

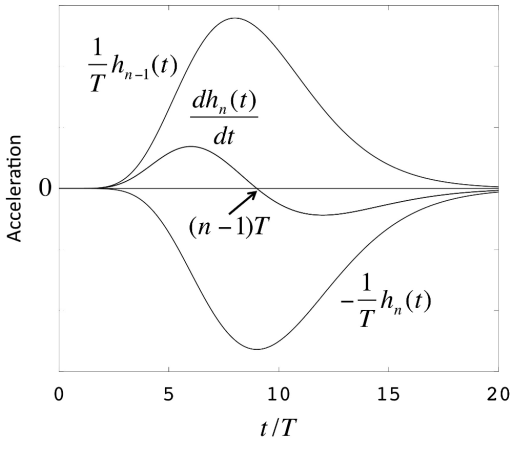

FIGURE 3. Visual description of the derivative of Equation (3) corresponding to the acceleration time pattern. An example is presented for a 10-th order cascade model.

Considering the time pattern of $dh_n(t)/dt$ illustrated in Figure 3, the waveform of the second-order derivative according to Equation (5) can be formed by combining the derivative pattern with the n-th order model, $-dh_n(t)/dt$ and the derivative pattern with the $(n-1)$-th order model, $dh_{n-1}(t)/dt$. This result suggests that the time pattern for the

n-th order derivative can be produced by overlapping the two $(n-1)$-th order derivatives of the response patterns of the n-th and $(n-1)$-th order cascade models. Therefore, the waveform of the derivative can be produced by pattern overlapping.

4.1.2. *Integration.* By integrating Equation (4) with respect to t, the following equation can be obtained:

$$\int h_n(t)dt = \int h_{n-1}(t)dt - Th_n(t) \tag{6}$$

If we use its recursive property, Equation (6) can be modified as:

$$\begin{aligned}\int h_n(t)dt &= \int h_1(t)dt - T\sum_{i=2}^{n} h_i(t) = \frac{A}{T}\int e^{-\frac{t}{T}}dt - T\sum_{i=2}^{n} h_i(t) \\ &= C - Ae^{-\frac{t}{T}} - T\sum_{i=2}^{n} h_i(t)\end{aligned} \tag{7}$$

where C represents the integration constant. If we assume initial values for Equation (7) $= 0$ at $t = 0$, then the constant is determined as $C = A$. Considering the relationship $A\exp(-t/T) = Th_1(t)$, the final result can be obtained as:

$$\int h_n(t)dt = A - T\sum_{i=1}^{n} h_i(t) \tag{8}$$

This result suggests that the integration of Equation (3) with respect to t contains the impulse response patterns of the cascade model ranging from the first-order to the n-th order.

Figure 4 presents a visual description of the integration of Equation (3) based on the relationship provided by Equation (8). As illustrated in the figure, the integration time pattern is formed by subtracting the n-th and lower-order impulse response patterns from the step-shaped time pattern, which has a value of A. Considering the dimensions of A, length, and T, time in Equation (8), the impulse response $h_n(t)$ corresponds to the dimension of length/time and is consistent with the idea in Equation (3), which corresponds to the velocity profile of articulatory behavior in Section 3.

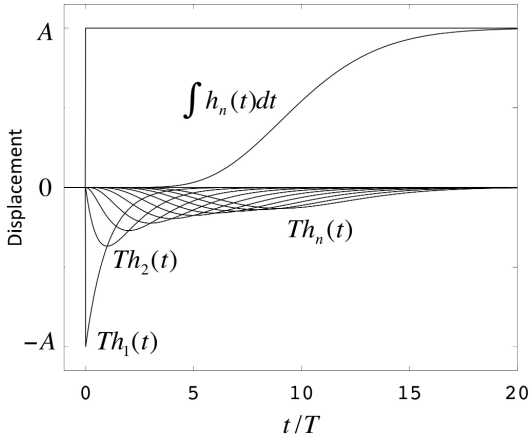

FIGURE 4. Visual description of the integration of Equation (3) corresponding to the displacement time pattern. An example is presented for a 10-th order cascade model.

5. **Application to the Gamma Function.** The previous section described the calculation method for the response patterns of the cascade model. This section describes the application of the calculation method to the gamma function.

If we consider the case where $A = 1$ and $T = 1$ in Equation (3), the following equation can be obtained:

$$t^{n-1}e^{-t} = (n-1)!h_n(t), \quad t \geq 0 \tag{9}$$

By integrating Equation (9) with respect to t over the interval $[a, b]$ and using Equation (8), the following result can be obtained.

$$\begin{aligned}\int_a^b t^{n-1}e^{-t}dt &= (n-1)!\int_a^b h_n(t)dt \\ &= (n-1)!\left[-\sum_{i=1}^{n} h_i(t)\right]_a^b = (n-1)!\sum_{i=1}^{n}(h_i(a) - h_i(b)) \\ &= (n-1)!\sum_{i=1}^{n}\left\{\frac{1}{(i-1)!}\left(a^{i-1}e^{-a} - b^{i-1}e^{-b}\right)\right\}\end{aligned} \tag{10}$$

This result suggests that the integration of Equation (9) with respect to t can be obtained by calculating the n-th and lower-order impulse responses based on Equation (3) with $A = 1$ and $T = 1$. In addition, the integration for any interval $[a, b]$ can be calculated using the last part of Equation (10).

For the case where $a = 0$ and $b = \infty$ in Equation (10), considering the shape of the impulse response patterns in Figure 1, the following relationship can be obtained.

$$\sum_{i=1}^{n}(h_i(0) - h_i(\infty)) = 1 \tag{11}$$

Therefore, the following final result is obtained:

$$\int_0^\infty t^{n-1}e^{-t}dt = (n-1)! \tag{12}$$

This relationship is well-known for a gamma function.

Although this relationship is obtained when $A = 1$ and $T = 1$ in Equation (3), the same result can be obtained for any T. This relationship also implies the following result in terms of the integration of $h_n(t)$ for any A:

$$\int_0^\infty h_n(t)dt = A \tag{13}$$

6. **Pattern Design Based on the Model.** In the previous sections, a model consisting of a cascaded first-order system and its properties were described. The visualization of the waveform patterns based on the calculation method is beneficial for an intuitive understanding of waveform modeling. In this section, the response patterns based on the model are presented to demonstrate the flexibility of the modeling method and validate its potential.

Before the presentation, related equations based on the model for displacement, velocity, and acceleration patterns are presented in Table 1. As described above, these patterns can be produced using impulse response patterns based on Equation (3). The parameters for designing the response patterns are presented in Table 2. The command input time T_{in} controls the location of the response pattern on the time axis as $h_n(t - T_{\text{in}})$.

Because basic waveform patterns for displacement, velocity, and acceleration based on a single impulse response $h_n(t)$ are shown in Figure 2, examples of combinations of two or

TABLE 1. Displacement, velocity, and acceleration patterns and their corresponding equations in the modeling method

Displacement pattern	Equation (8)
Velocity pattern	Equation (3)
Acceleration pattern	Equation (4)

TABLE 2. Parameters for designing the response patterns based on Equation (3)

n	Order
A	Amplitude
T	Time constant
T_{in}	Command input time

more impulse response patterns based on the models are presented here to demonstrate the basic behavior of the synthesized patterns by considering the effects of the values of the parameters in Equation (3). In the figures in this section, the horizontal axis as the time axis is normalized by the time constant T, as illustrated in Figure 1. The values of the parameters are different depending on the application fields. The purpose of the simulation here is to show the flexibility of the modeling by pattern overlapping; basically, normalized values are used for generality. In Figure 8, in which three response patterns are involved, the parameter values, particularly for the time constant, were determined as similar values by referring to the experimental results in [2].

6.1. **Effects of the order.** Figure 5 illustrates synthesized waveform patterns (black) generated from two impulse response patterns with opposite movement directions such as ascending (blue) and descending (magenta) movements in displacement. These opposite movements are produced from two cascade models, each of which activates the movement in each direction. Each model consists of n units of a first-order component, as presented in Figure 1. The vertical bars with numbers 1 and 2 represent the command input times of the step inputs to the models. The response patterns are accompanied by the numbers such as (1) and (2) corresponding to the input command numbers. The effects of the order of the models on the waveform patterns are shown for three cases of the n order: 4, 6, and 10. The three vertically aligned patterns correspond to the displacement, velocity, and acceleration waveform patterns, respectively. As can be observed, the smoothness of the waveform patterns increased in that order. Because differentiation is sensitive to local changes in the waveform, the acceleration and velocity waveforms depict the details of the synthesized waveforms even when the displacement waveforms are relatively similar, as illustrated in Figures 5(a)-5(c).

6.2. **Effects of the time constant.** Figure 6 illustrates synthesized waveform patterns generated from two impulse response patterns with opposite movement directions. The time constant effects of the models on the waveform patterns are demonstrated for three cases of the time constant T: $0.5T$, T, and $1.5T$. In these examples, a 10-th order model was adopted because it was used in [2]. The time constant controls the duration of the phenomena, i.e., the horizontal scaling of a waveform pattern along the time-axis. The change in the smoothness of the waveform patterns as the time constant changes is similar to the case of the order mentioned above. The order of the model affects the shape of the waveform pattern, as illustrated in Figure 1, whereas the time constant affects the speed of the change in the waveform pattern.

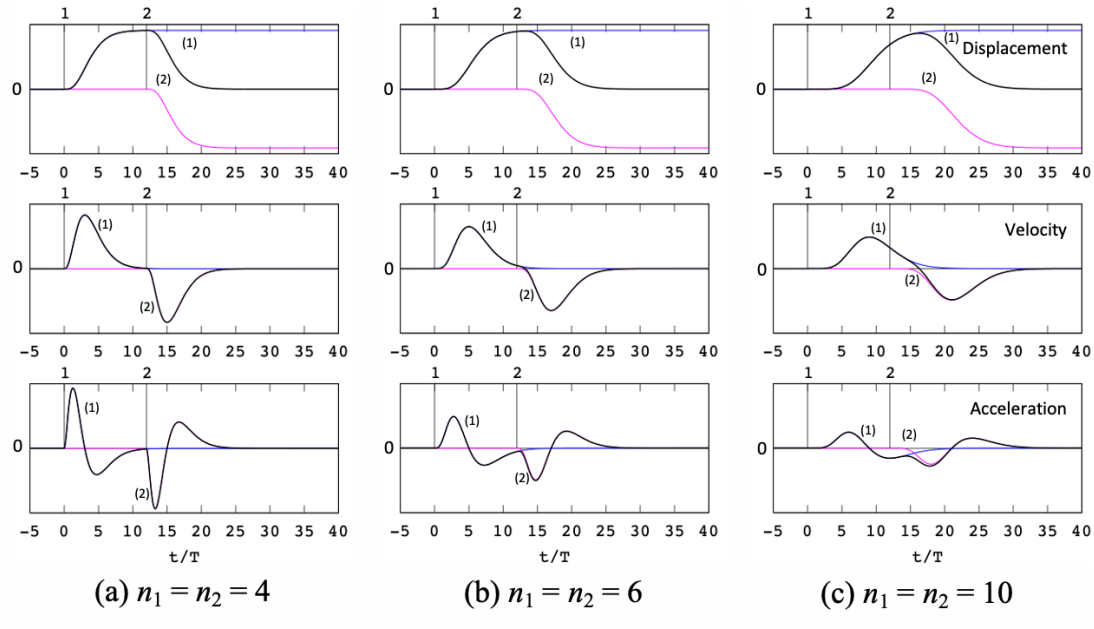

FIGURE 5. (color online) Effects of the order of the models on the synthesized waveform patterns generated from two impulse response patterns with opposite movement directions ($A_1 = A$, $A_2 = -A$, $T_1 = T_2 = T$, $T_{\text{in1}} = 0$, $T_{\text{in2}} = 12$). The vertical bars with numbers 1 and 2 represent the command input times of the step inputs to the models. The response patterns are accompanied by the numbers such as (1) and (2) corresponding to the input command numbers for considering monochrome print.

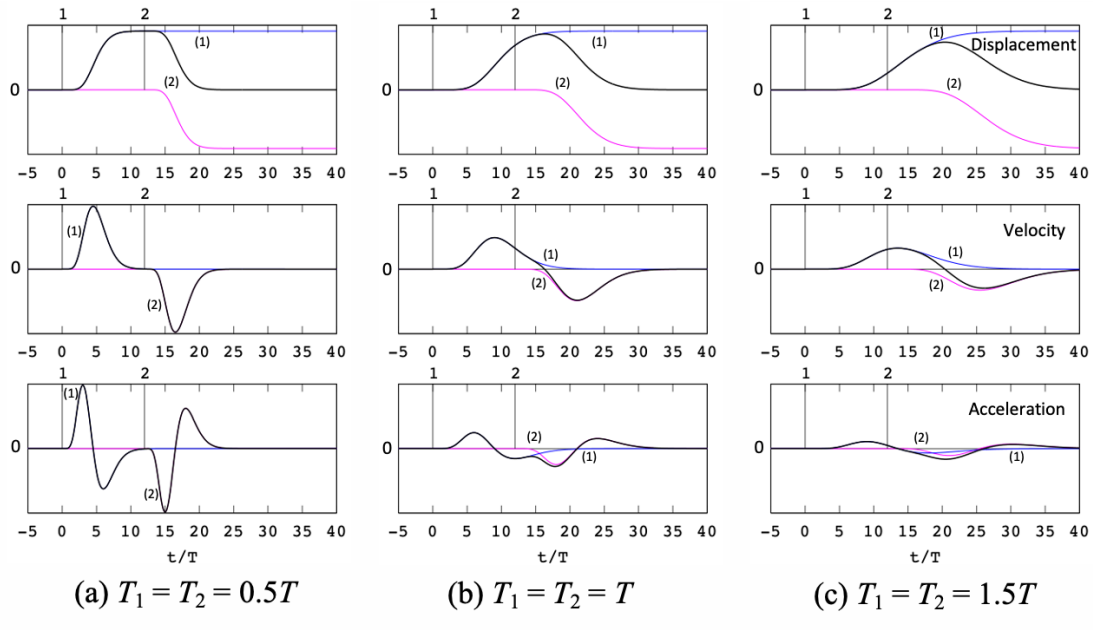

FIGURE 6. (color online) Effects of the time constant of the models on the synthesized waveform patterns generated from two impulse response patterns with opposite movement directions ($n_1 = n_2 = 10$, $A_1 = A$, $A_2 = -A$, $T_{\text{in1}} = 0$, $T_{\text{in2}} = 12$)

6.3. **Effects of the overlapping time interval.** Figure 7 illustrates synthesized waveform patterns generated from two impulse response patterns with opposite movement directions. The effects of overlapping the response patterns of the models on the waveform patterns are shown for three cases with intervals of 4, 8, and 12. The cases shown in Figures 7(a) and 7(b) have relatively long overlapping portions, and their acceleration patterns have a negative peak, whereas the case shown in Figure 7(c) has two negative peaks in its acceleration pattern.

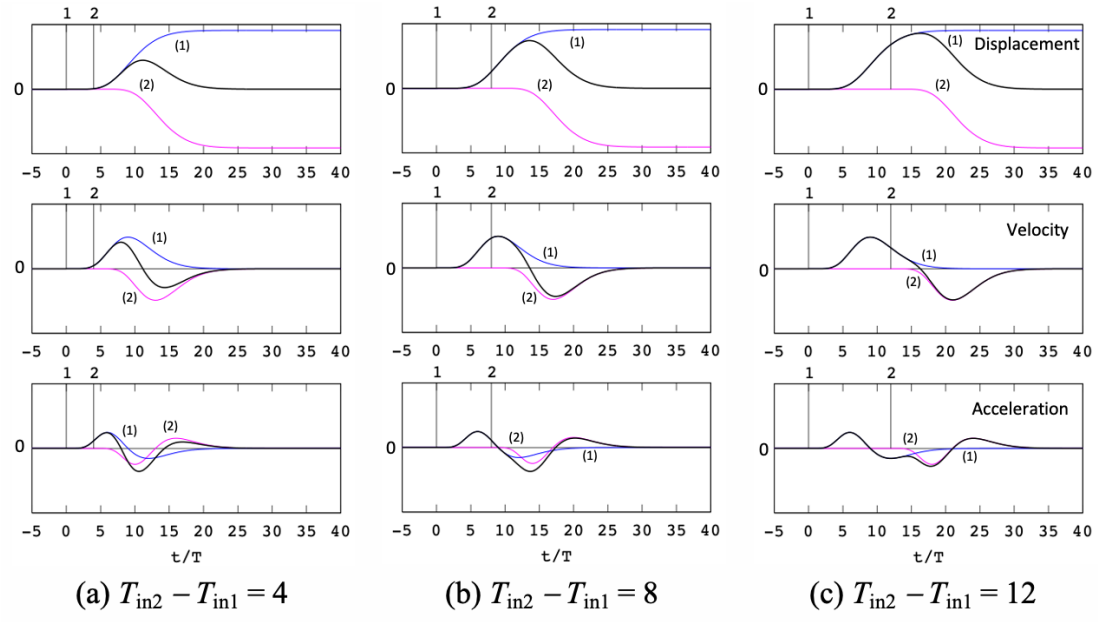

FIGURE 7. (color online) Effects of overlapping the response patterns from the models on the synthesized waveform patterns generated from two impulse response patterns with opposite movement directions ($n_1 = n_2 = 10$, $A_1 = A$, $A_2 = -A$, $T_1 = T_2 = T$)

6.4. **Effects of the overlapping of the multiple response patterns.** Figure 8 presents the examples of the synthesized waveform patterns generated from three impulse response patterns. In each example, the synthesized waveform pattern (black) consists of two short-term response patterns corresponding to ascending (blue, (1)) and descending (magenta, (2)) movements and a long-term response pattern corresponding to a descending movement (green, (0)) as a trend. In other words, the synthesized waveform pattern is a mixture of short- and long-term movement patterns. This situation is based on the idea that articulatory movement /eda/ consists of a long-term trend for the /ea/ vowel sequence and short-term ascending and descending movements for stop consonant /d/ at the blade of the tongue in speech production [2].

In Figure 8, the effects of the timing of overlapping the long-term descending movement with short-term ascending and descending movements on the synthesized waveform patterns are illustrated. These examples are obtained by considering the situation in which the parameters for two impulse response patterns corresponding to the short-term movements are fixed and the timing of the overlap of the long-term movement is sliding along the time-axis. In the figure, the input times for the two impulse responses are indicated as 1 and 2, and that for the long-term movement is indicated as 0. The timing of the overlap was gradually delayed, and its effects are shown in Figures 8(a)-8(e). In Figure 8(a), the long-term descending movement occurs at the beginning of the ascending

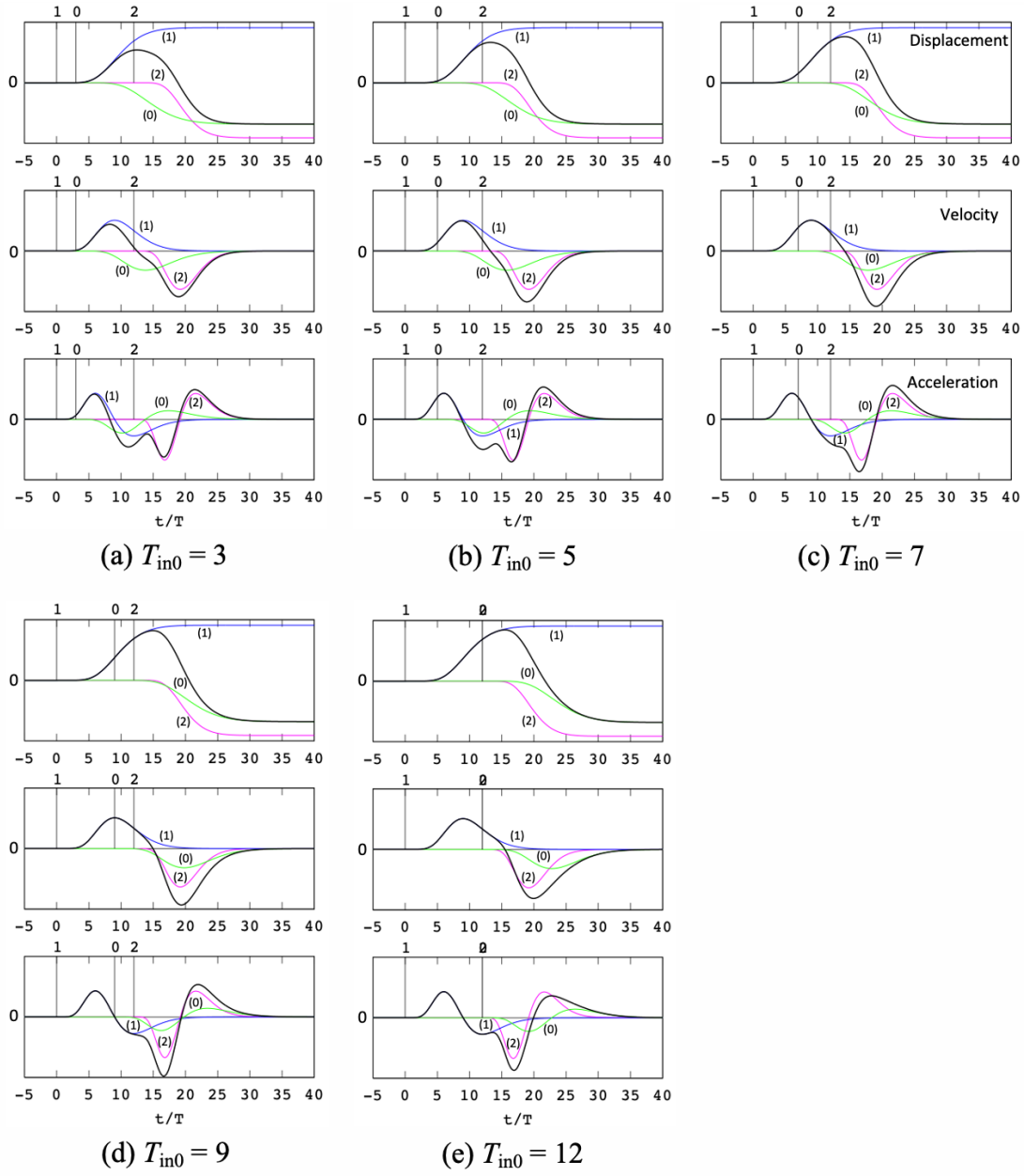

FIGURE 8. (color online) Effects of the timing of overlap on the synthesized waveform patterns generated from three impulse response patterns ($n_1 = n_2 = 10$, $A_1 = A$, $A_2 = -A$, $T_1 = T$, $T_2 = 0.8T$, $T_{in1} = 0$, $T_{in2} = 12$, $n_0 = 10$, $A_0 = -0.75A$, $T_0 = 1.2T$)

movement generated by the first impulse response pattern, and the resulting ascending movement cannot reach its maximum level of displacement. This effect can be observed as the first negative peak in acceleration. As the timing of the overlap is gradually delayed, as illustrated in Figures 8(b)-8(e), the synthesized velocity pattern exhibits a large negative value during the descending movement; consequently, a large negative value can be observed at the second negative peak in acceleration. Thus, smooth displacement patterns can be generated by overlapping waveform patterns generated from several impulse response patterns.

Basic sample programs written in the Octave language [12] for displaying the synthesized waveform patterns are provided in the Appendix.

Figure 9 presents an example of the modeling of waveform patterns for articulatory movements as a reference from [2]. In this example, the observed and calculated movement patterns for the tongue during the utterance /edade/ are shown for the displacement, velocity, and acceleration with the speech sound wave. The calculated movement patterns are based on the waveform pattern model described above and are expressed as a combination of a long-term trend for the /ea/ vowel sequence and short-term ascending and descending movements for stop consonant, /d/, for the /eda/ portion, as well as for the /ade/ portion. The time instants $t_{\mathrm{d}}^{\mathrm{u}}$ and $t_{\mathrm{d}}^{\mathrm{d}}$ correspond to the input times for the short-term ascending and descending movements for stop consonant /d/, respectively, and t_{a} corresponds to the input times for the long-term trend for the /ea/ vowel sequence, as shown in Figure 8(b). As can be seen, the calculated movement patterns closely match the observed ones, and the waveform patterns for the /eda/ portion are very similar to those shown in Figure 8(b) in terms of displacement, velocity, and acceleration.

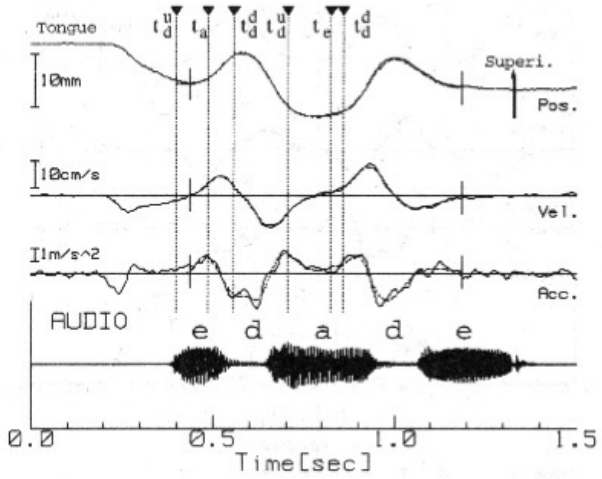

Observed (—) and calculated (···) movement patterns for the tongue during the utterance /edade/.

FIGURE 9. Example of the modeling of waveform patterns for articulatory movements [2]

7. **Discussion.** The differentiation and integration of the impulse response can be directly performed by numerical calculations using Equation (3). However, the relationships given by Equations (4) and (8), and related Figures 3 and 4 clarify the recursive structure of the related time response patterns and visual meaning. By focusing on the relationships, the related time patterns can be calculated by combining the impulse response patterns based on Equation (3). Thus, Equation (3) acts as a core function that produces a fundamental pattern for designing various time patterns by combining the fundamental patterns with different orders.

The effectiveness of the cascade model has been reported in several studies [2, 3, 4, 5, 6]. The calculation method shown in this study revealed the visual meaning of the modeling results and the interesting property that when the model is used as an approximation for high-order systems, the related time patterns, such as the displacement, velocity, and acceleration patterns, can be considered as overlapping with the impulse response patterns.

The outcomes of this study can be summarized as follows:

- Properties of the response pattern of the cascaded first-order components are described and the calculation method for its differentiation and integration is provided by focusing on its recursive structure;
- Considering the impulse response pattern as a velocity profile, that is, velocity waveform pattern of movement, the waveform patterns for the displacement and acceleration can also be calculated based on the impulse response pattern;
- The smoothness of the response patterns can be controlled by the values for the order and the time constant of the cascade model;
- Complex waveform patterns can be generated by combining several impulse response patterns and controlling the timing of their overlap;
- A modeling method based on the pattern overlapping has application examples for articulatory movements.

In [2], a 10-th order model was adopted considering the approximation accuracy and reaction time of biological systems [13]. Birkholz et al. [6] also stated that a 10-th order model has a reaction time of approximately 50-100 ms, which matches [14, 15]. However, the command does not always mean a physiological command; in this model, an input signal to the model is a hypothetical command to activate the response pattern as an output signal. However, it can be a useful timing command to produce the desired waveform pattern. Indeed, hypothetical commands for appropriate superposition timing regarding articulatory gestures between vowels and consonants for vowel-consonant-vowels (VCV) were investigated in a simulation study [16].

The property of the kinematics of arm movement is one of the most well-studied topics [17, 18, 19, 20, 21]. In these studies, bell-shaped velocity profiles for arm movement trajectories were reported, and a minimum-jerk model [18] and a minimum torque-change model [19] have been proposed. Because our modeling method based on the cascade model also produces waveform patterns with bell-shaped velocity profiles, the patterns may be applicable to core response patterns for the study of trajectory planning. A relatively recent study [22] introduced continuing efforts to obtain optimization models for the trajectory planning of human movements. This suggests the importance of trajectory planning with a low calculation cost and smooth movement patterns.

As described above, in our modeling method, pattern overlapping can produce a new waveform pattern, and the resulting pattern can maintain its smoothness as a function of time. This also means that additional commands as compensatory commands can be introduced to adapt the situation change caused by disturbances or changes in the goal in displacement.

The shapes of the tangential velocity profiles of the observed vertical arm movements shown in [23] are similar to the impulse response patterns with relatively higher orders, as shown in Figure 1, that is, an asymmetrical shape in which the duration of negative acceleration after the velocity peak is longer than that for positive acceleration before the peak, as shown in Figure 2. In contrast, opposite shapes, that is, the duration after the velocity peak is slightly shorter than that before the peak can be seen in Figure 3 in [18] and Figure 3 in [19]. Such velocity profiles can also be produced based on the overlapping idea shown in Figure 7. Figure 10 illustrates such an example. By adding an opposite response pattern (magenta, (2)) at the ending stage of the original single response pattern (blue, (1)), a similar response pattern (black) can be produced, as shown in Figure 10(b). In this case, the added opposite response pattern acts as a brake. Thus, the modeling method is flexible because it locates response patterns on the time axis, that is, mapping response patterns on the time axis.

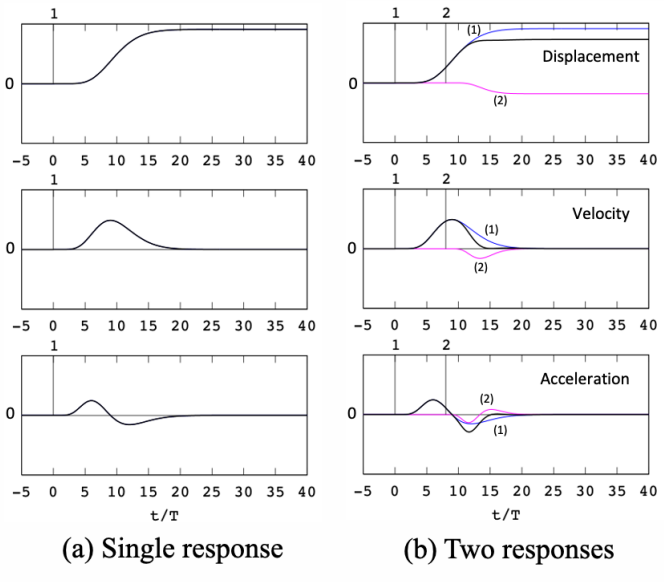

FIGURE 10. (color online) Effects of adding a response pattern to the original single response pattern on the synthesized waveform pattern ($n_1 = n_2 = 10$, $A_1 = A$, $A_2 = -0.2A$, $T_1 = T$, $T_2 = 0.6T$, $T_{\text{in1}} = 0$, $T_{\text{in2}} = 8$)

8. **Conclusions.** As demonstrated in this study, a model comprising a cascaded first-order system exhibits interesting properties. In this case, the differentiation and integration of its impulse response with respect to time can be realized based on a combination of impulse response patterns. These properties suggest that the impulse response pattern based on the cascade model is a fundamental component pattern for representing trajectory patterns as a function of time, such as the displacement, velocity, and acceleration. Given that the cascade model has the potential to approximate the transfer functions for high-order systems, it would be beneficial for articulatory movements, as well as for other movements, such as locomotion in biological systems. This study focused on the properties of the cascade model and the visualization of the waveform patterns based on the impulse response. The findings of this study provide a new perspective on modeling high-order systems, including the possibility of applying waveform modeling for displacement, velocity, and acceleration to various cases, and the response patterns of the model work as useful cores or kernel patterns to represent, decompose, and design response patterns of systems.

Applied research using the response patterns based on the model in this study, such as efficient waveform matching between the observed data and the model responses, and movement trajectory planning, movement prediction is the next step for future work.

Acknowledgment. Part of this work was supported by a Grant-in-Aid for Scientific Research JP17K06464 from the Japan Society for the Promotion of Science.

REFERENCES

[1] J. H. Milsum, *Biological Control Systems Analysis*, McGraw-Hill, New York, 1966.
[2] K. Ogata and Y. Sonoda, Modeling of articulatory dynamics using cascaded first-order systems, *Journal of the Acoustical Society of Japan*, vol.55, no.3, pp.156-164, 1999 (in Japanese).
[3] K. Ogata and Y. Sonoda, Evaluation of articulatory dynamics and timing based on cascaded first-order systems, *Proc. of the 5th International Seminar on Speech Production: Models and Data and CREST Workshop on Models of Speech Production: Motor Planning and Articulatory Modelling*, pp.321-324, 2000.

[4] K. Ogata and Y. Sonoda, Quantitative analysis of articulatory behavior based on cascaded first-order systems, *Acoustical Science and Technology*, vol.23, no.2, pp.117-120, 2002.
[5] K. Ogata and Y. Sonoda, Reproduction of articulatory behavior based on parameterization of articulatory movements, *Acoustical Science and Technology*, vol.24, no.6, pp.403-405, 2003.
[6] P. Birkholz, B. Kröger and C. Neuschaefer-Rube, Model-based reproduction of articulatory trajectories for consonant-vowel sequences, *IEEE Trans. Audio, Speech, and Language Processing*, vol.19, no.5, pp.1422-1433, 2011.
[7] K. Pearson, On lines and planes of closest fit to systems of points in space, *Philosophical Magazine*, vol.2, no.11, pp.559-572, 1901.
[8] I. T. Jolliffe, *Principal Component Analysis*, Springer-Verlag, New York, 1986.
[9] T. W. Lee, *Independent Component Analysis: Theory and Applications*, Kluwer Academic Publishers, Boston, 1998.
[10] A. Hyvärinen, J. Karhunen and E. Oja, *Independent Component Analysis*, John Wiley & Sons, Inc., New York, 2001.
[11] T. Ishibashi and K. Eguchi, Blind source separation for human speeches based on orthogonalization of joint distribution of observed mixture signals, *ICIC Express Letters, Part B: Applications*, vol.12, no.5, pp.443-451, 2021.
[12] *GNU Octave*, https://www.gnu.org/software/octave/, Accessed on Apr. 3, 2021.
[13] K. Matsunami, *Motion and Brain*, Kinokuniya Shoten, Tokyo, 1986 (in Japanese).
[14] P. J. Alfonso and T. Baer, Dynamics of vowel articulation, *Language and Speech*, vol.25, no.2, pp.151-173, 1982.
[15] R. Netsell and B. Daniel, Neural and mechanical response time for speech production, *Journal of Speech and Hearing Research*, vol.17, no.4, pp.608-618, 1974.
[16] K. Ogata and K. Nakashima, Analysis of articulatory timing based on a superposition model for VCV sequences, *2014 IEEE International Conference on Systems, Man, and Cybernetics (SMC)*, pp.3720-3725, 2014.
[17] N. Hogan, An organizing principle for a class of voluntary movements, *Journal of Neuroscience*, vol.4, no.11, pp.2745-2754, 1984.
[18] T. Flash and N. Hogan, The coordination of arm movements: An experimentally confirmed mathematical model, *Journal of Neuroscience*, vol.5, no.7, pp.1688-1703, 1985.
[19] Y. Uno, M. Kawato and R. Suzuki, Formation and control of optimal trajectory in human multijoint arm movement, *Biological Cybernetics*, vol.61, pp.89-101, 1989.
[20] Y. Koike and M. Kawato, Trajectory formation from surface EMG signals using a neural network model, *IEICE Trans. D-II*, vol.J77-D-II, no.1, pp.193-203, 1994 (in Japanese).
[21] M. Kawato, *Computational Theory of Brain*, Sangyo Tosho Publishing, Tokyo, 1996 (in Japanese).
[22] Y. Uno, Optimization models of human movements, *Journal of the Robotics Society of Japan*, vol.32, no.6, pp.525-529, 2014 (in Japanese).
[23] C. G. Atkeson and J. M. Hollerbach, Kinematic features of unrestrained vertical arm movements, *Journal of Neuroscience*, vol.5, no.9, pp.2318-2330, 1985.

Appendix A. **Basic Sample Programs Written in the Octave Language.** Basic sample programs written in the Octave language to display the synthesized waveform patterns are provided as a reference. The sample comprises a script file and three function files called from the script, and expressed as:

- Calc_response_CFS.m
- h_CFS.m
- h_diff_CFS.m
- h_integral_CFS.m

The details of each file are provided below. The programs were written with priority on comprehensibility.

A.1. **Sample script file for displaying synthesized patterns.**

Contents of Calc_response_CFS.m

```
# display synthesized patterns based on the cascade model
```

```
# by K. Ogata

  clear all;
  close;

  figure (1, 'position', [100 100 480 720]);

  T0 = 1.2;
  A0 = -0.75;
  Tin0 =  3.0;
  n0 = 10;

  T1 = 1.0;
  A1 = 1.0;
  Tin1 = 0.0;
  n1 = 10;

  T2 = 0.8;
  A2 = -1.0;
  Tin2 = 12.0;
  n2 = 10;

  t = -5:0.1:50;

  for i=1:columns(t)
    zero_line(i) = 0;
  endfor

# for Velocity
  for i=1:columns(t)
    h0(i) = h_CFS(n0, A0, T0, (t(i)-Tin0));
    h1(i) = h_CFS(n1, A1, T1, (t(i)-Tin1));
    h2(i) = h_CFS(n2, A2, T2, (t(i)-Tin2));
  endfor
  h_total = h0 + h1 + h2;

# for Acceleration
  for i=1:columns(t)
    h0_diff(i) = h_diff_CFS(n0, A0, T0, (t(i)-Tin0));
    h1_diff(i) = h_diff_CFS(n1, A1, T1, (t(i)-Tin1));
    h2_diff(i) = h_diff_CFS(n2, A2, T2, (t(i)-Tin2));
  endfor
  h_diff_total = h0_diff + h1_diff + h2_diff;

# for Displacement
  for i=1:columns(t)
    h0_integral(i) = h_integral_CFS(n0, A0, T0, (t(i)-Tin0));
    h1_integral(i) = h_integral_CFS(n1, A1, T1, (t(i)-Tin1));
    h2_integral(i) = h_integral_CFS(n2, A2, T2, (t(i)-Tin2));
  endfor
  h_integral_total = h0_integral + h1_integral + h2_integral;

  set(gca, "fontsize", 40);

# for Displacement
  subplot(3, 1, 1);
  hold on;
  plot(t, h2_integral, '4', "linewidth",2);
```

```
  plot(t, h1_integral, '3', "linewidth",2);
  plot(t, h0_integral, '2', "linewidth",2);
  plot(t, h_integral_total, '-0', "linewidth",3);

  ytop = 1.1;
  ybot = 0.0;
  plot([Tin0,Tin0], [ytop, ybot], '0', "linewidth",1);
  text(Tin0 - 0.6, ytop + 0.2, '0');
  plot([Tin1,Tin1], [ytop, ybot], '0', "linewidth",1);
  text(Tin1 - 0.6, ytop + 0.2, '1');
  plot([Tin2,Tin2], [ytop, ybot], '0', "linewidth",1);
  text(Tin2 - 0.6, ytop + 0.2, '2');
  axis([-5 40 -1.1 1.1], 'ticx');

# for Velocity
  subplot(3, 1, 2);
  hold on;
  plot(t, zero_line, '0', "linewidth",1);
  plot(t, h2, '4', "linewidth",2);
  plot(t, h1, '3', "linewidth",2);
  plot(t, h0, '2', "linewidth",2);
  plot(t, h_total, '0', "linewidth",3);

  ytop = 0.26;
  ybot = 0.0;
  plot([Tin0,Tin0], [ytop, ybot], '0', "linewidth",1);
  text(Tin0 - 0.6, ytop + 0.04, '0');
  plot([Tin1,Tin1], [ytop, ybot], '0', "linewidth",1);
  text(Tin1 - 0.6, ytop + 0.04, '1');
  plot([Tin2,Tin2], [ytop, ybot], '0', "linewidth",1);
  text(Tin2 - 0.6, ytop + 0.04, '2');
  axis([-5 40 -0.26 0.26], 'ticx');

# for Acceleration
  subplot(3, 1, 3);
  hold on;
  plot(t, zero_line, '0', "linewidth",1);
  plot(t, h2_diff, '4', "linewidth",2);
  plot(t, h1_diff, '3', "linewidth",2);
  plot(t, h0_diff, '2', "linewidth",2);
  plot(t, h_diff_total, '0', "linewidth",3);

  ytop = 0.08;
  ybot = 0.0;
  plot([Tin0,Tin0], [ytop, ybot], '0', "linewidth",1);
  text(Tin0 - 0.6, ytop + 0.014, '0');
  plot([Tin1,Tin1], [ytop, ybot], '0', "linewidth",1);
  text(Tin1 - 0.6, ytop + 0.014, '1');
  plot([Tin2,Tin2], [ytop, ybot], '0', "linewidth",1);
  text(Tin2 - 0.6, ytop + 0.014, '2');
  axis([-5 40 -0.08 0.08], 'ticx');

  xlabel('t/T');

  print -depsc "-S480,720" figurefile.eps;
```

A.2. **Function file for calculating the impulse response.**

Contents of h_CFS.m

```
function retval = h_CFS(n, a, T, t)
# calculate h(t) = a exp(-t/T)(t/T)^(n-1)/((n-1)!T)

  if (nargin != 4)
    usage ("h_CFS(n, a, T, t)");
  endif;

  m = 1:(n-1);
  yfact = prod(m);

  if (t >= 0)
    retval =  a * exp(-t/T) .* (t/T)^(n-1) ./ (yfact * T);
  else
    retval =  0;
  endif

endfunction
```

A.3. **Function file for calculating the differentiation of the impulse response.**

Contents of h_diff_CFS.m

```
function retval = h_diff_CFS(n, a, T, t)
# calculate d hn(t)/dt = (1/T){-hn(t)+h(n-1)(t)}

  if (nargin != 4)
    usage ("h_diff_CFS(n, a, T, t)");
  endif;

  if  (t >= 0)
    retval =  (-h_CFS(n, a, T, t) + h_CFS(n-1, a, T, t)) / T;
  else
    retval =  0;
  endif

endfunction
```

A.4. **Function file for calculating the integration of the impulse response.**

Contents of h_integral_CFS.m

```
function retval = h_integral_CFS(n, a, T, t)
# calculate  {Integral}hn(t)dt = a-T{Sigma i=1 to n}hi(t) + C

  if (nargin != 4)
    usage ("h_integral_CFS(n, a, T, t)");
  endif;

  c = 0;
  sum = 0;
  for i=1:n
    sum = sum + h_CFS(i, a, T, t);
  endfor
```

```
  if (t >= 0)
    retval =  a - T * sum + c;
   else
    retval =  0;
  endif

endfunction
```